frontiers in Earth Science

ORIGINAL RESEARCH
published: 23 November 2021
doi: 10.3389/feart.2021.747675

Experimental Study on Gangue Backfilling Materials Improved by Soda Residue and Field Measurement of Surface Subsidence

Wei Yin[1,2]*, *Kun Zhang*[1,2], *Shenyang Ouyang*[3], *Xiaomin Bai*[4], *Wenjie Sun*[1] and *Jingru Zhao*[1]

[1]The Key Laboratory for Traffic and Transportation Security of Jiangsu Province, Huaiyin Institute of Technology, Huaian, China, [2]Huai'an Zhongbo Traffic Safety Technology Co., Ltd, Huaian, China, [3]School of Mines, China University of Mining and Technology, Xuzhou, China, [4]Faculty of Mechanical and Material Engineering, Huaiyin Institute of Technology, Huaian, China

In coal mining, the problems of massive discharge of solid waste, environmental pollution, and surface subsidence disaster are urgent to be solved. Based on this engineering background, the feasibility of using solid waste soda residue to improve gangue cemented backfilling material was discussed, and the surface subsidence of the test working face was measured in this study. Besides, the influence of soda residue on the performance of gangue cemented backfilling materials was analyzed through laboratory tests. The experimental results show that 1) as the content of soda residue increases within the range of 0–12%, the slump of the soda residue gangue backfilling material (SRGBM) slurry gradually increases, and the bleeding rate increases. The early strength and later strength of SRGBM increase first and then decrease with the increase in soda residue content. 2) The optimal ratio of the soda residue cemented backfilling material is soda residue: fly ash: lime: cement: gangue = 6%: 34%: 10%: 2.5%: 47.5%. Compared with the reference group, the slump of the material is increased by 12.7%, the bleeding rate is only 3.8%, and the early strength and later strength are increased by 449 and 187%, respectively. 3) The addition of soda residue promotes the hydration reaction of the slurry system of soda residue cemented materials. The coexistence of C-S-H gel and N-A-S-H gel reduces the connectivity of pores and improves the strength of the material. 4) The maximum surface subsidence of the test working face is only 245 mm, and the surface subsidence control effect is good. Therefore, the preparation of SRGBM with soda residue can achieve energy saving and emission reduction, with significant technical, economic, and social benefits, and has good promotion and application value.

Keywords: soda residue, cemented fill mining, transport property, mechanical properties, strength mechanism, surface subsidence

OPEN ACCESS

Edited by:
Qingsheng Bai,
Freiberg University of Mining and Technology, Germany

Reviewed by:
Di Wu,
University of Science and Technology Beijing, China
Mohammed Ashfaq,
National Institute of Technology Warangal, India

***Correspondence:**
Wei Yin
yinweihyit@163.com

Specialty section:
This article was submitted to Geohazards and Georisks, a section of the journal Frontiers in Earth Science

Received: *26 July 2021*
Accepted: *19 October 2021*
Published: *23 November 2021*

Citation:
Yin W, Zhang K, Ouyang S, Bai X, Sun W and Zhao J (2021) Experimental Study on Gangue Backfilling Materials Improved by Soda Residue and Field Measurement of Surface Subsidence. Front. Earth Sci. 9:747675. doi: 10.3389/feart.2021.747675

INTRODUCTION

Coal is the basic energy in China. However, the traditional caving mining method causes surface collapse disaster in a large area and solid waste discharge of gangue, which seriously damages the ecological environment of mining areas (Zhang et al., 2020; Ma et al., 2021a). Statistically, about 795 million tons of solid waste gangue is discharged annually in China, and about 6.56×10^8 m^2 of land subsidence is caused (He et al., 2015), which severely restricts the sustainable development of mines

in China. Cemented fill mining has the advantages of surface subsidence reduction, gangue emission reduction, and environmental protection and has become the core technology of green mining systems (Martin And Holger, 2013; Deng et al., 2020; Meng et al., 2017). Cemented backfilling can be divided into low-concentration tailings cemented backfilling, high-concentration full-tailings cemented backfilling (Zhao et al., 2011), high water quick setting tailings cemented backfilling (Guangming et al., 2010), paste cemented backfilling (Zhou et al., 2019), and waste rock cemented backfilling (Li et al., 2020a; Liu et al., 2020; Meng et al., 2020). Backfilling material (Ma et al., 2019a) is the key to cemented backfilling, and the material cost accounts for more than 40% of the backfilling cost (Liu et al., 2021). The gangue-based cemented backfilling mainly composed of gangue and fly ash (solid waste) has been widely applied (Cui and Henghu, 2010; Wang et al., 2019; Ran et al., 2020). Studies on the performance of gangue-based cemented materials (including slump, diffusivity, rheological properties, setting time, compressive strength, shear strength, and material mix proportion) have been widely performed (Li et al., 2020b; Yin et al., 2020a; Yin et al., 2020b). With the development of deep mining (Ma et al., 2021b), the mining environment of high ground stress and high ground temperature is frequently encountered; the proper disposition of bulk solid waste and cost reduction of backfilling materials are urgently required (Zhang et al., 2018). Consequently, higher requirements are put forward for the performance of cemented backfilling materials and cost control of backfilling mining (Ma et al., 2020a).

Soda, renowned as "the mother of chemical industry," has been widely used in construction, chemical industry, textile, and other industries. The output of soda ash in China ranks first in the world, mainly based on the ammonia-soda process (Song et al., 2019). According to statistics, 0.3–0.6 t solid waste of soda residue is discharged for every 1 t of soda ash produced (Sun et al., 2012). Due to the high alkalinity and high chloride ion content of soda residue, the traditional ground discharge method not only occupies a large number of land resources but also causes soil salinization (Yang et al., 2017a). From the perspective of environmental protection and land resource utilization, the scientific treatment of solid waste soda residue has become a problem faced by salt chemical enterprises (Hulisz and Piernik, 2013; Yang et al., 2017b). Mitchell (Mitchell, 1993) in Japan mixed soda residue with fly ash to make engineering soil for road reclamation. Xu Dong et al. (Xu et al., 2020) used soda residue, slag, steel slag, and desulfurization gypsum as composite cementing materials, tailings sand, and waste rock as aggregates to prepare clinker-free concrete. Yan Shuwang (Yan et al., 2006) mixed soda residue and calcium ash in a certain proportion and made soda residue soil for site backfilling. Morgan (Morgan, 1996) and Huang Lanfen (Lanfen et al., 2014) used the alkalinity of soda residue to improve acid soil. Yang Jiujun (Yang et al., 2010) used soda residue as an admixture to partially replace fly ash for the preparation of building mortar. The above utilization method consumes the solid waste of soda residue to a certain extent. However, due to the low strength of soda residue itself and the existence of chloride in soda residue, the phenomenon of spreading soda and corrosion of steel bar appears in the engineering (Ma et al., 2020b). Consequently, the existing soda residue treatment methods hardly meet the comprehensive requirements of the project on bearing capacity, anti-deformation, environmental protection, and large-scale treatment at the same time (Ma et al., 2019b).

Research has found that soda residue contains alkalinity (Tian and Li, 2009) and a large number of $CaCO_3$, $Ca(OH)_2$, and other components, which can be used to improve the performance of cement concrete to a certain extent (Tan et al., 2018). Due to the non-chlorine corrosion of the filling body (no reinforcement is used inside the backfill) and the rising price of fly ash, the technical idea of using soda residue to replace part of fly ash and preparing soda residue gangue backfilling material (SRGBM) is germinated. In this study, the basic characteristics of soda residue, gangue, fly ash, and other raw materials were tested, and SRGBM with different soda residue contents was prepared. The slump, bleeding rate, and uniaxial compressive strength of SRGBM at different ages were analyzed. The influence of soda residue content on the flow performance and mechanical properties of SRGBM was investigated, and the strength formation mechanism of SRGBM was explored. The proposed SRGBM was applied to engineering in the test mine, and the surface subsidence measurement was performed to verify the control effect of SRGBM on the surface subsidence of the mining area. This study provides a reference for the large-scale resource treatment of solid waste soda residue and the development and performance improvement of new cemented backfilling materials.

GANGUE CEMENTED FILL MINING AND PERFORMANCE INDEX

Technical Principle

In the gangue cemented fill mining, gangue is used as an aggregate, and the additives (such as fly ash) and cementing materials (such as cement, lime) are added. Then, water is added in the ground or underground mixing station to obtain paste slurry by mixing. Subsequently, the slurry is transported to the underground goaf by gravity or backfilling pump through the transportation channel such as drilling or pipeline, and then the excess water is removed from the slurry in the goaf (or dehydration is omitted). After the slurry solidifying strength is improved, the slurry is used to support the surrounding rock, fill the goaf, and control the overburden movement and surface deformation. The principle of gangue cemented fill mining technology is shown in **Figure 1**.

Performance Index Analysis of Soda Residue Gangue Backfilling Material

SRGBM is formed by gangue with certain gradation, lime, cement, fly ash, and other materials mixed with water. As the main bearing body of goaf, the cemented backfilling materials go through the flowing state and solidification state of the slurry. The ideal SRGBM needs to have two core indexes of good transport property and mechanical property at the same time. In addition, it should also meet the requirements of wide sources, low cost, and no contaminants in engineering.

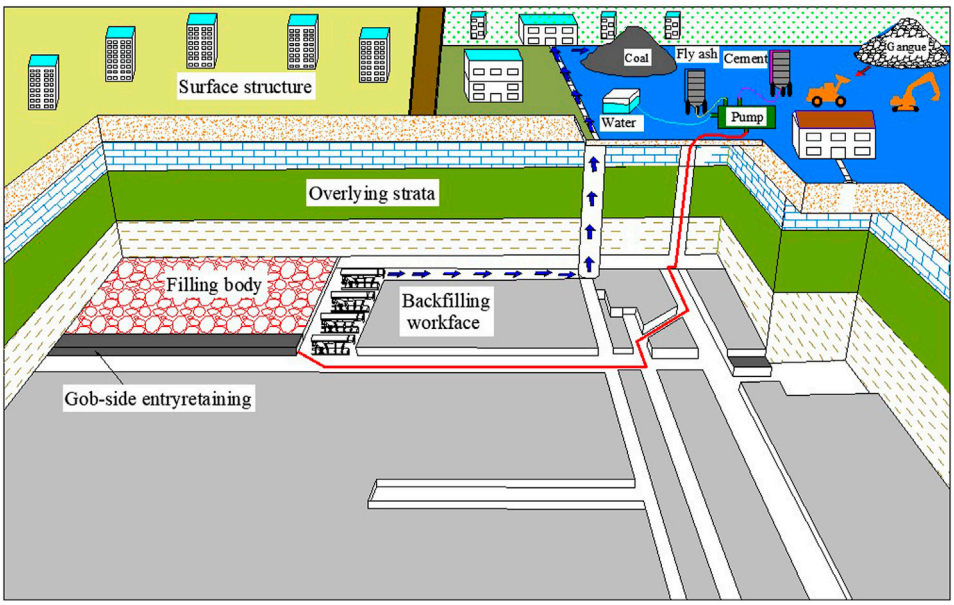

FIGURE 1 | Technical principle of cemented fill mining.

Transport Properties

Slump

The transport property determines the difficulty and effect of transportation of backfilling slurry to the underground goaf. A poor transport property will lead to plugging of the backfilling pipeline. Slump directly reflects the workability, fluidity, and pump ability of cemented backfilling materials (Yu et al., 2016), which is usually used as a direct index to evaluate the transport property of the backfilling slurry. Engineering practice has proved that the slump of the backfilling slurry meeting the transportation requirements should not be less than 100 mm, and it has good transport properties when the slump is 120–200 mm (Shenyang, 2019).

Bleeding Rate

Bleeding rate is another index to measure the transport property of the backfilling slurry, which reflects the water retention and segregation degree of slurry. The larger the bleeding rate, the more serious the slurry segregation and the worse the transport property. Consequently, pipe plugging can be easily caused in the pumping process. Besides, the cement and other fine particles in the slurry can be easily brought out during the bleeding process, which reduces the strength of the material in the later stage (Wang et al., 2014). The practice has shown that the bleeding rate of the backfilling slurry meeting the requirements of transport property should be less than 5% (Shenyang, 2019).

Mechanical Properties

The mechanical properties of the backfilling materials determine the controlling effect of the filling body on the overburden after solidification. The higher the mechanical strength of backfilling materials, the stronger the bearing capacity of the filling body. According to the function of the cemented filling body in different periods of goaf, the mechanical properties can be divided into early strength and later strength.

Early Strength

During the backfilling mining, cemented backfilling materials must be self-supporting without collapse after backfilling into goaf. Therefore, SRGBM needs to have early strength, that is, the strength required for the filling body to maintain self-supporting at the early stage. Although the early strength requirement is not high, it is of great significance for backfilling mining. The early strength design methods include the empirical formula and Thomas model (Wang, 2019). Considering the actual backfilling technology in a coal mine, the unconfined compressive strength (UCS) of the filling body at the curing age of 1 day is selected as the early strength index. The relationship between the early strength and the backfilling height of the goaf is shown in the following equation:

$$h^2 = k\sigma_z^3, \tag{1}$$

where h is the height of the filling body, m; k is the empirical coefficient of early strength, and $k = 600$ generally; and σ_z is the early strength of the cemented filling body, MPa.

Later Strength

With the internal hydration reaction of the cemented backfilling slurry, the strength of the cemented filling body gradually increases and finally tends to be stable. In the goaf, the filling body is used to support the overburden, and the strength at the curing age of 28 days is generally taken as the later strength in the research. In this study, the control of surface subsidence is taken as the backfilling target. If the strength of the filling body needs to control the main key strata of overburden without breaking, then the later strength of the filling body needs to control the weight of

FIGURE 2 | Composition materials of SRGBM: **(A)** gangue, **(B)** soda residue, **(C)** fly ash, **(D)** lime, and **(E)** cement.

rock strata between the immediate roof and the main key strata. The later strength calculation is shown in the following equation:

$$\sigma_h = a\sum_{i=1}^{n} r_i h_i, \tag{2}$$

where σ_h is the later strength of cemented filling body, MPa; n is the number of strata between the direct roof of overburden and the main key strata; h_i is the thickness of the ith layer, m; r_i is the unit weight of the ith layer, MN/m^3; and a is the safety factor of later strength, ranging from 1.1 to 1.4.

MATERIALS AND METHODS

Materials

The original gangue-based cemented backfilling material used in the test mine was taken as the reference group. The mix proportion of raw materials in the reference group was gangue: fly ash: cement: lime = 47.5%: 40%: 10%: 2.5%, and the mass concentration of the slurry was 84%. In recent years, there is a supply tension of fly ash in the market, and the price of fly ash is rising gradually. In this study, the technical idea of using soda residue to replace fly ash was proposed. Based on the reference group, SRGBM was prepared by replacing fly ash with soda residue in proportion. **Figure 2** shows the actual photos of raw materials.

Soda Residue

The test soda residue was taken from Huai'an Soda Plant. The fresh soda residue was a gray sticky paste with a pungent smell and strong corrosion. The soda residue was dried by natural air drying, and the moisture content, pH value, liquid plastic limit, UCS, and other basic parameters of the air-dried soda residue were tested according to Test Methods of Soils for Highway Engineering (JTG E40-2007). The chemical composition of soda residue was analyzed by XRF tests. **Table 1** shows basic physical and mechanical parameters and chemical components of soda residue.

The moisture content of soda residue was 89.95%, the pH value was 9.2, and it was alkaline. The plasticity index was 29.53, belonging to high liquid limit clay. The UCS value of soda residue was only 0.20 MPa, indicating the low strength of soda residue. The scanning electron microscope (SEM) was used to scan the internal structure of air-dried soda residue. **Figure 3** shows the internal structure under different magnifications. Based on the analysis, the soda residue was a porous aggregate structure. It was inferred that the material skeleton of soda residue was mainly formed by $CaCO_3$, and the single-particle size was about 2–5 μm. The particles were cemented with each other to form aggregates. Due to the main point contact of particles, the cementation of the soda residue was weak. The surface of the aggregate structure was rough, and there were many pores of different sizes on the surface and inside of particles, resulting in the high water content and large bearing deformation in a natural state.

Gangue

The test gangue was taken from the washing gangue of the coal preparation plant. The natural moisture content of the gangue was 6.7% and the density was 1.9 g/cm^3. The gangue was ground into a powder specimen and tested by a D/max-3B X-ray diffractometer. The main components of gangue are quartz and kaolinite, and the total amount of both is more than 70%; there are also some illite and illite/smectite formations, amorphous materials, and a small number of other minerals.

Gangue has a high content of SiO_2 and can act as the material skeleton, contributing to better deformation resistance of backfilling materials. Besides, gangue also contains carbon, aluminum, and Cao, which is easy to react with fly ash. **Figure 4** shows the SEM micrographs of the internal structure of gangue under different resolution conditions.

According to **Figure 4A**, there are many holes on the surface of gangue, the surface joints and fissures are developed, the coarse and fine particles are cemented with each other, there are obvious edges and corners at the end of the particles, and the fracture is flat. After magnification of 6000 times (**Figure 4B**), the micro-layered structure of fractures can be clearly found; the rock specimens are stacked in sheets, and the sheets are

TABLE 1 | Physical and mechanical parameters and chemical composition of soda residue.

Physical and mechanics parameters				Chemical component/%					
No	Item	Value	Unit	No	Compositions	Content	Number	Compositions	Number
1	Moisture content	89.95	%	1	CaO	52.25	6	MgO	2.33
2	PH	9.2	-	2	SO_3	16.97	7	Al_2O_3	1.76
3	Plastic limit	53.96	%	3	Cl	18.39	8	Fe_2O_3	1.17
4	Liquid limit	83.49	%	4	SiO_2	4.06	9	K_2O	0.15
5	UCS	0.20	MPa	5	NaO_2	2.46	10	Others	0.46

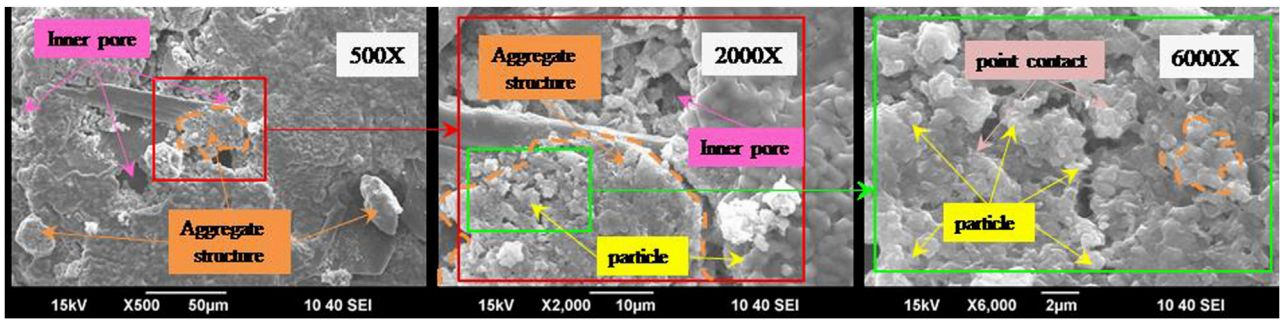

FIGURE 3 | SEM micrographs of microstructure inside soda residue at different magnification.

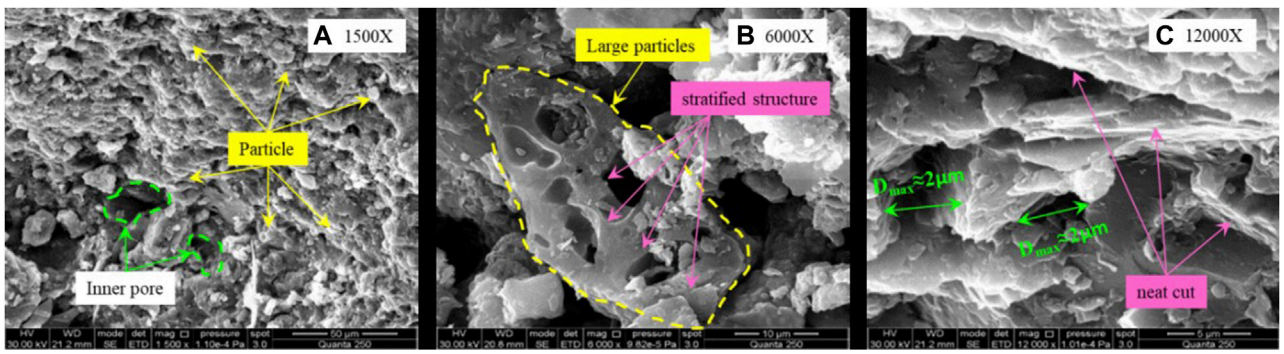

FIGURE 4 | SEM micrographs of gangue at different magnification: **(A)** 1500x, **(B)** 6000x, and **(C)** 12000x.

crisscrossed. After magnification of 12000 times (**Figure 4C**), the microscopic pores are distributed on the surface of gangue, and the diameter of pores is about 2 μm. SEM results show that gangue itself has good density and can be used as an aggregate component of cemented backfilling materials.

Fly Ash

The fly ash used in the test was from the spontaneous combustion coal power plant. According to the analysis, the main oxide components in fly ash are SiO_2, Al_2O_3, Fe_2O_3. The Al_2O_3, and SiO_2, which account for 74% are the favorable component of fly ash activity and are closely related to the later setting and hardening characteristics of cemented backfilling materials (Papadakis, 1999).

According to SEM micrographs of fly ash, fly ash particles have different particle sizes and shapes. There are more particles with small sizes and fewer particles with large sizes; most of the particle size is 10–20 μm, and the maximum particle size is about 170 μm. It is observed that many pores are evenly distributed on its surface, and there are small flake structures locally.

Cement

The cement used in this test was P.O.32.5 cement produced by China United Cement Company. The apparent density of the cement was 3.1 g/cm^3, and 80 μm sieve residual was 6.4%. The analysis shows that there are a lot of tricalcium silicate (C_3S), dicalcium silicate (C_2S), part of tricalcium aluminate (C_3A), and tetracalcium ferroaluminate (C_4AF) in cement. After hydration of cement, calcium silicate hydrate and ettringite with cementing ability can be produced. The results of the mineral composition analysis are shown in **Table 2**.

TABLE 2 | Mineral composition of cement.

Compositions	C_3S	C_2S	C_3A	C_4AF	Other
Content (%)	1.5	1.2	25.5	48.8	Rest

Lime

The lime used in this test was quicklime produced by Huihui Industrial Company. Through the analysis, it is found that the main components of lime are calcium oxide and calcium hydroxide, accounting for 70%. Calcium oxide is a kind of nonhydraulic cementing material, which has poor cementing ability in the water environment. The addition of lime can stimulate the activity of fly ash, promote the hydration process of fly ash, and improve the strength of the filling body; Besides, the calcium oxide contained in lime can react with water, consume free water content, and reduce slurry bleeding rate.

Test Scheme

To study the influence of soda residue content on the flow and mechanical properties of SRGBM, five groups of tests (groups A0—A4) were designed. Group A0 was the reference group without soda residue. The specific ratios are available in Chapter 3.1. The amount of soda residue in groups A0–A4 was 0, 3, 6, 9, and 12% respectively, and the corresponding quality of fly ash in each group decreased. Slump and bleeding rate are specific indexes of flow performance. Early strength, middle strength, and later strength are mechanical property indexes in this test, corresponding to the UCS at the curing age of 1, 7, and 28 days. **Table 3** shows the test proportioning scheme and monitoring indexes.

Sample Preparation and Test Process

After grinding the soda residue in advance, raw materials in different groups were mixed according to the test scheme. Then, an appropriate amount of tap water was added to stir to form cemented backfilling slurry. The slump and bleeding rate of slurry were tested according to the GB/T 50080–2016 Standard for test method of performance on ordinary fresh concrete. During the bleeding rate test, the water exuded from the surface was sucked by the straw at an interval of 10 min in the first 60 min; after 60 min, the water was sucked every 30 min until there was no more water on the surface. The mechanical properties were tested with a triple die (7.07 × 7.07 × 07 cm) for mold mounting, and then the mold was removed after 24 h. The mold was cured under the standard curing condition (at the temperature of 20°C and the humidity of 95%) at the curing age of 1, 7, and 28 days. The WAW-1000D electro-hydraulic servo press was selected to test the UCS of the cemented filling body at different curing ages. The loading speed was set as 1 mm/s. Three specimens were tested at each age, and the average value was taken as the final result. The actual pictures of the test process are shown in **Figure 5**.

RESULTS AND DISCUSSION

Flow Performance

Slump

Figure 6 shows the slump test results of the SRGBM slurry with different soda residue contents in Groups A0–A4.

As shown in **Figure 6**, when the soda residue content is 0, 3, 6, 9, and 12%, the slump values of slurry are 110, 115, 124, 135, and 152 mm, respectively. It indicates that the slump value of slurry gradually increases with the increase in soda residue content. Compared with the reference group (Group A0), the increase in the slump value in Groups A1–A4 is 4.5, 12.7, 22.7, and 38.2%, respectively, and the increasing amplitude gradually increases with the increase in soda residue content. The reason is as follows: there is a large number of fine particles of soda residue after grinding and the water content is high, which increases the slump value of slurry and enhances the fluidity of the backfilling material.

Bleeding Rate

Figure 7 shows test results of bleeding and bleeding rate of slurry with different contents of soda residue.

As shown in **Figure 7A**, the bleeding law of the SRGBM slurry in each group presents two-stage characteristics of rapid bleeding (stage I) and slow bleeding (stage II). In stage I, the speed of bleeding is faster and the bleeding proportion is larger in the whole process, while in stage II, the speed of bleeding is slower and the bleeding proportion is smaller in the whole process. The bleeding proportion of stage I in the reference group (Group A0) is as high as 98% and that of stage I in Group A4 is 91%. With the increase in soda residue content, the final bleeding in stage II increases gradually, but the proportion of bleeding in stage I decreases gradually. It indicates that soda residue can delay the initial bleeding rate of free water, which is conducive to material transportation.

As presented in **Figure 7B**, when the soda residue contents are 0, 3, 6, 9, and 12%, the bleeding rate of slurry in Groups A0–A4 is 2.4, 3.0, 3.8, 4.7, and 5.3%, respectively. The bleeding rate

TABLE 3 | Test proportioning scheme and monitoring index.

Group	Solids content composition (wt%)					Mass Concentration (%)	Monitoring index				
	Soda residue	Fly ash	Cement	Lime	Gangue		Slump	Bleeding rate	UCS (1 day)	UCS (7 days)	UCS (28 days)
A0	0	40	10	2.5	47.5	84	s_0	b_0	σ_{01}	σ_{02}	σ_{03}
A1	3	37	10	2.5	47.5	84	s_1	b_1	σ_{11}	σ_{12}	σ_{13}
A2	6	34	10	2.5	47.5	84	s_2	b_2	σ_{21}	σ_{22}	σ_{23}
A3	9	31	10	2.5	47.5	84	s_3	b_3	σ_{31}	σ_{32}	σ_{33}
A4	12	28	10	2.5	47.5	84	s_4	b_4	σ_{41}	σ_{42}	σ_{43}

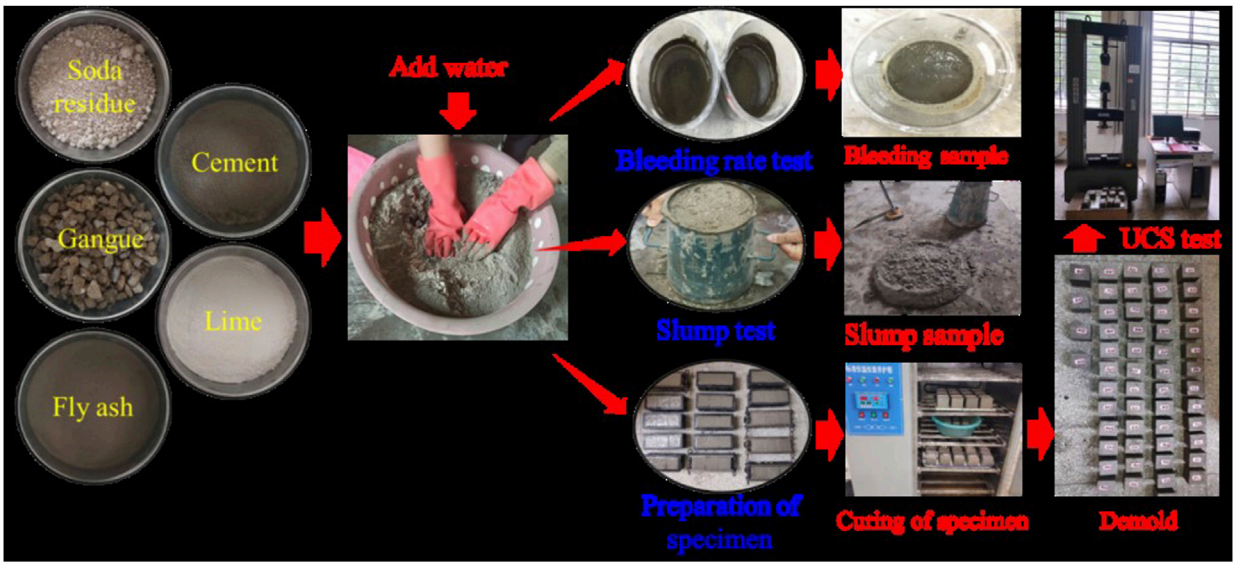

FIGURE 5 | Actual pictures of the test process.

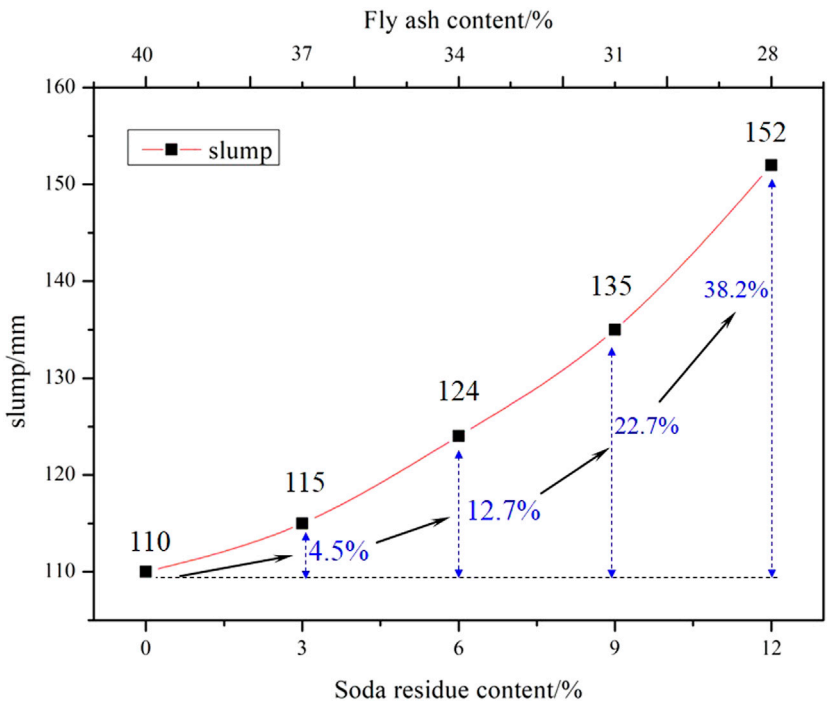

FIGURE 6 | Influence law of slump.

gradually increases with the increase in soda residue content. The increasing amplitude of the bleeding rate of slurry in Groups A1–A4 is 25, 58, 95, and 120%, respectively. This increasing amplitude is significant, and the bleeding rate of slurry in Group A4 is too large, which has exceeded the recommended value. The analysis shows that the water absorption rate of fly ash with the same quality is higher than that of soda residue; the water absorbed by soda residue is less than the water demand of fly ash; the free water of slurry is more, which leads to the increase in bleeding rate.

Mechanical Properties

Bearing Deformation Characteristics

One specimen was selected from three specimens at different curing ages in Groups A0–A4 and subject to the loading. The

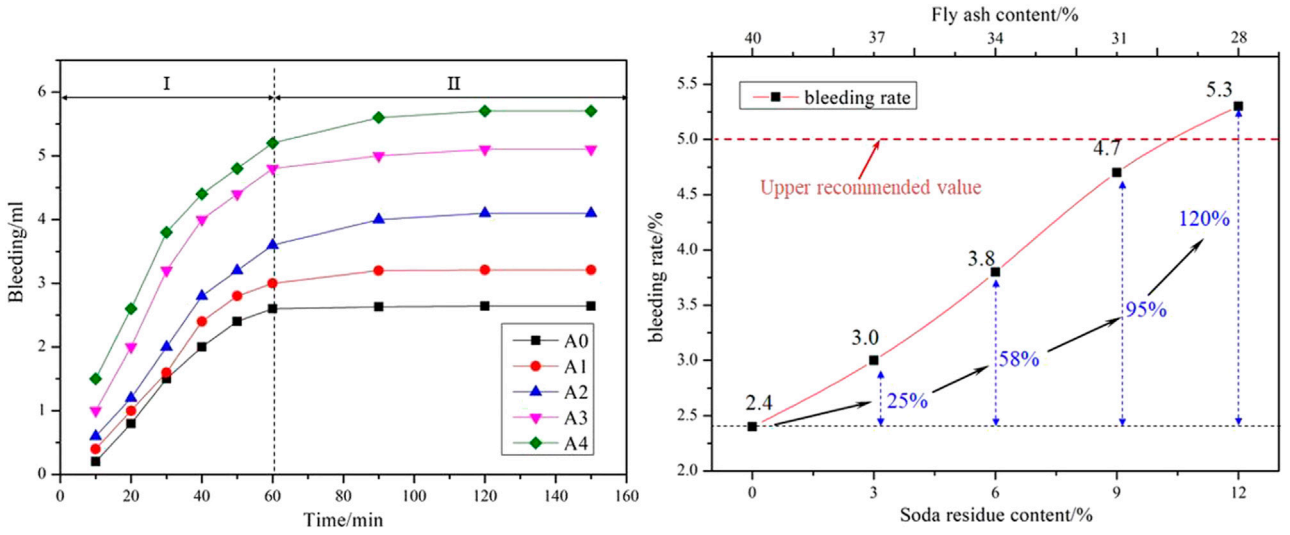

FIGURE 7 | Curves of bleeding and bleeding rate of the backfilling slurry.

stress–strain curve of SRGBM specimens was drawn, as shown in **Figure 8**.

As shown in **Figure 11**, the strength curves of SRGBM specimens with different soda residue contents and different ages show significant three-stage characteristics, namely, pre-peak bearing area (zone I), post-peak attenuation area (zone II), and residual bearing area (zone III). In zone I, the strength of the specimen almost increases linearly with the increase of load. At the peak point, the specimen is in the ultimate strength, and the bearing capacity is the strongest. Zone I belongs to the strain hardening stage. In zones II and III, with the continuous action of the load, the strength of the specimen decreases rapidly, the bearing capacity becomes weak, the cracks continue to develop and connect, and the residual bearing area shrinks. However, the specimen in zone III does not completely lose the bearing capacity. It indicates that the material still has a certain bearing capacity after failure, but the bearing capacity is weak. Zones II and III belong to the strain-softening stage.

Analysis of Influence Characteristics

The UCS values of SRGBM specimens with different soda residue contents and ages were summarized. To further analyze the influence of soda residue content and curing age on the UCS of SRGBM specimens, the data are plotted as shown in **Figure 9**.

Curing age

As shown in **Figure 9A**, the UCS of SRGBM specimens with different soda residue contents increases gradually with the increase in curing time. The early strength and later strength of SRGBM in Group A2 are the largest, and the average uniaxial UCS of SRGBM at the curing age of 1, 7, and 28 days are 0.74, 3.95, and 12.54 MPa, respectively. The average UCS of the specimen at the curing age of 7 days is 5.3 times of that at the curing age of 1 day; the average UCS of the specimen at the curing age of 28 days is 16.9 times of that at the curing age of 7 days.

Soda residue content

As shown in **Figure 9B**, the UCS of SRGBM specimens increases first and then decreases with the increase in soda residue content. The strength of SRGBM at different curing ages is the highest at the soda residue content of 6%. Compared with the reference group, the UCS of SRGBM specimens at the curing ages of 1, 7, and 28 days in Group A2 is 5.49, 2.23, and 2.87 times of that in Group A2 (reference group), respectively. Based on the test results, it is suggested that the optimum mix proportion of SRGBM is soda residue: fly ash: lime: cement: gangue = 6%: 34%: 10%: 2.5%: 47.5%, and the slurry concentration is 84 wt%.

Strength Formation Mechanism

The cured specimen was broken and a small rectangular specimen with a base area of 10 × 10 mm and a height of 2–10 mm was cut from the inside of the specimen. The conductive adhesive was glued to the base and sprayed with gold to improve the electrical conductivity. Finally, the specimen was observed in the electron microscope. **Figure 10** shows the production process and the actual photos of the experiment. **Figure 11** shows the micrographs of SRGBM specimens under different resolution conditions.

According to the analysis of Chapter 3.1.4, the main components of cement are C_3A and C_4AF. The pH value and temperature of the solution are increased by the Cao in lime and water heating, and then trisulfide hydrated calcium sulfate ($3CaO{\cdot}Al_2O_3{\cdot}3CaSO_4{\cdot}32H_2O$, known as ettringite, expressed by Aft) is generated byC_3A. The reaction formula is shown in the following equations:

$$3CaO \cdot Al_2O_3 + Ca(OH)_2 \rightarrow 4CaO \cdot Al_2O_3 \cdot 13H_2O, \quad (3)$$

$$4CaO \cdot Al_2O_3 \cdot 13H_2O + 4CaSO_4 \cdot 2H_2O + H_2O \rightarrow 3CaO \cdot Al_2O_3 \cdot 3CaSO_4 \cdot 32H_2O. \quad (4)$$

When the gypsum is exhausted, calcium aluminate hydrate (C_4AH_{13}), which is the hydration product of C_3A, reacts with AFt

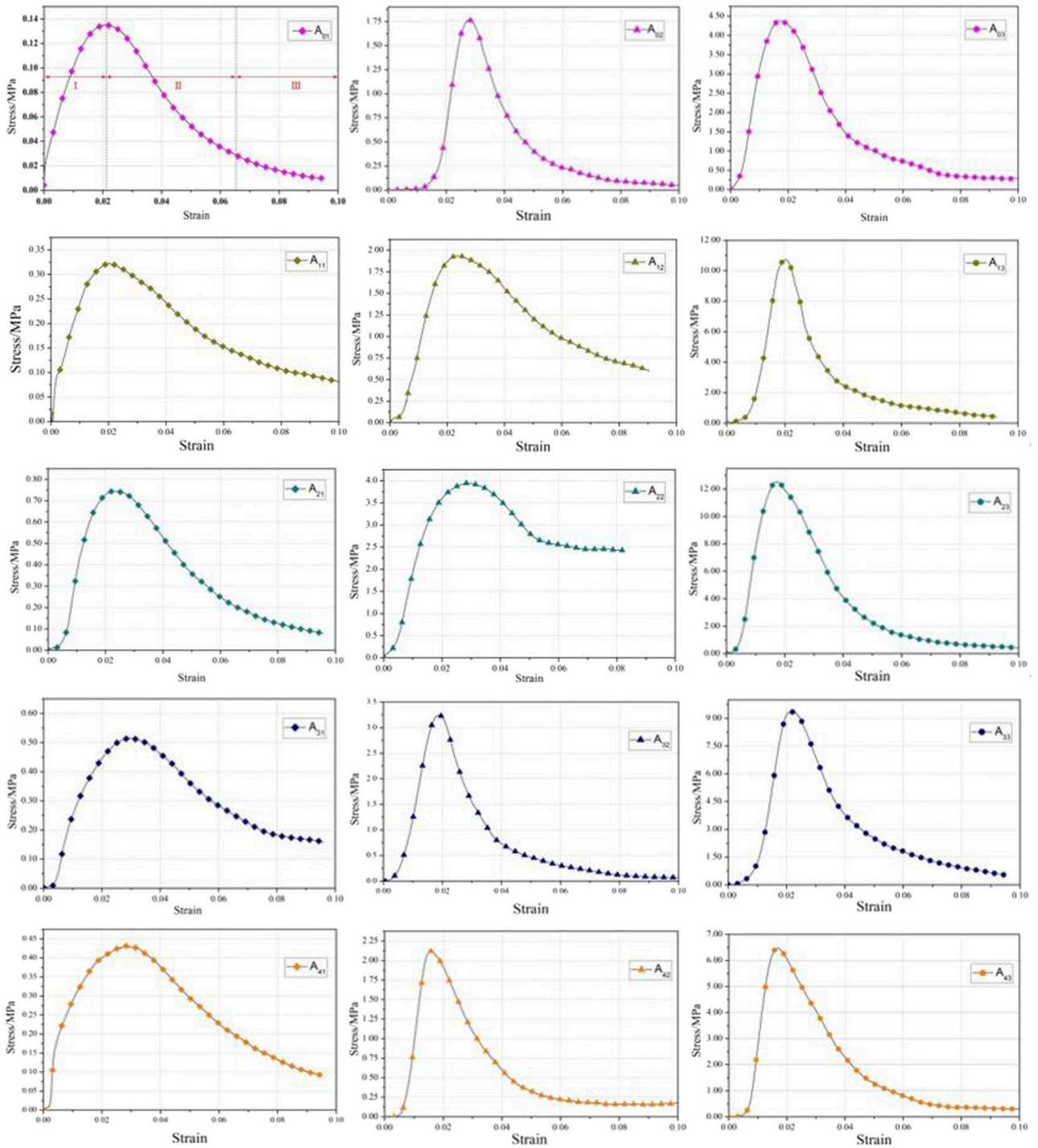

FIGURE 8 | Stress–strain curves of SRGBM specimens.

to form calcium sulphoaluminate hydrate ($3CaO{\cdot}Al_2O_3{\cdot}CaSO_4{\cdot}12H_2O$, expressed as AFm). Both of these hydrates are needle-like crystals and are insoluble in water. The reaction equations are shown in the following equations:

$$3CaO \cdot Al_2O_3 + 6H_2O \rightarrow 3CaO \cdot Al_2O_3{\cdot}6H_2O, \quad (5)$$

$$4CaO \cdot Al_2O_3{\cdot}13H_2O + 3CaO \cdot Al_2O_3{\cdot}3CaSO_4{\cdot}32H_2O \rightarrow 3CaO \cdot Al_2O_3{\cdot}CaSO_4{\cdot}12H_2O. \quad (6)$$

At the same time, fly ash is activated in the sodane environment of lime, the hydration reaction of cement is very rapid, and the

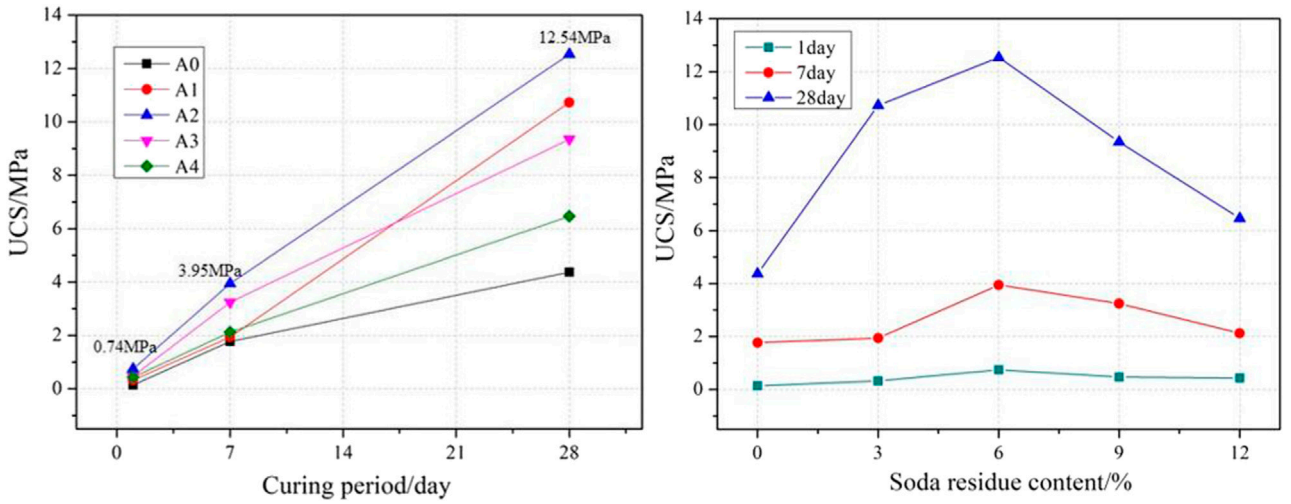

FIGURE 9 | Characteristic curve of strength influence.

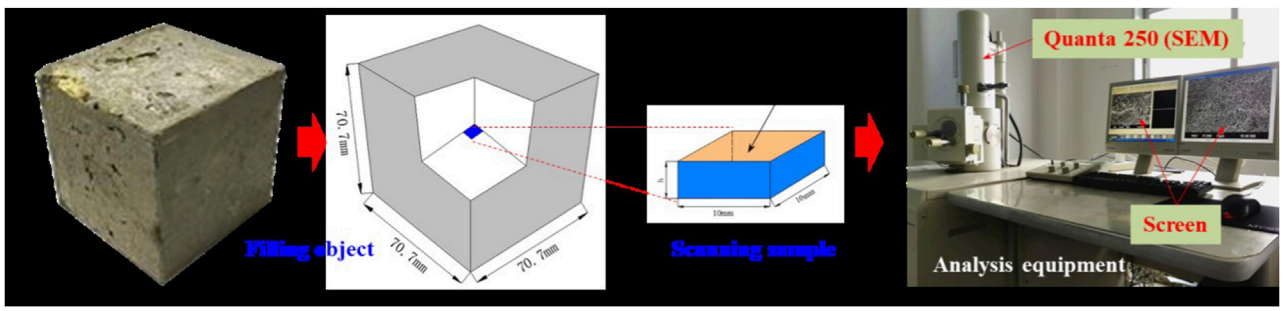

FIGURE 10 | SEM specimen preparation and actual photographing.

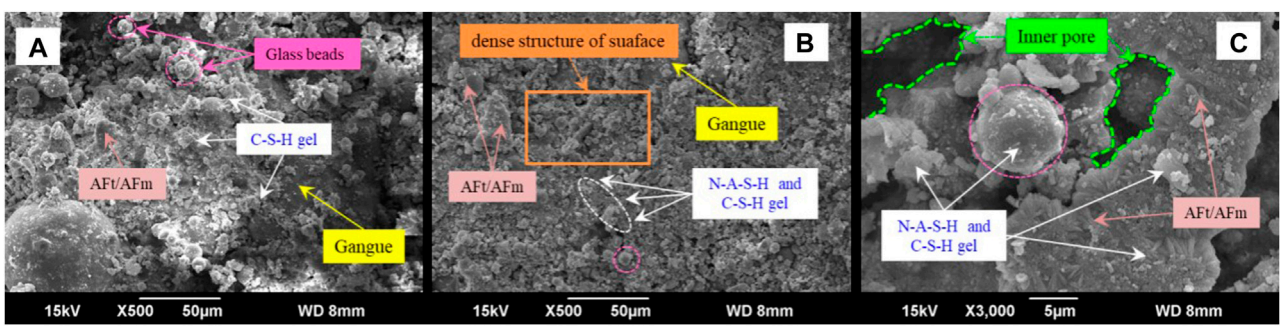

FIGURE 11 | SEM micrographs of the SRGBM internal structure.

released substances make the pH value of the solution further increase. The substances in fly ash have the characteristics of modifying the system structure, such as Ca^{2+}, K^{+}, and Na^{+}; silicate or aluminosilicate minerals are also dissolved in the solution. These substances with the ability of modifying the system structure contact with each other to form calcium silicate cement (C-S-H) and calcium aluminate hydrate (C_4AH_{13}). These hydration products can increase the structural density and strength of cemented backfilling materials and make the materials have a higher bearing capacity.

With the addition of soda residue, the active SiO_2 and Al_2O_3 contained in fly ash are excited by the OH^{-} contained in soda residue. After the dissolution and re-polymerization with different structures, aluminosilicate cementitious polymer

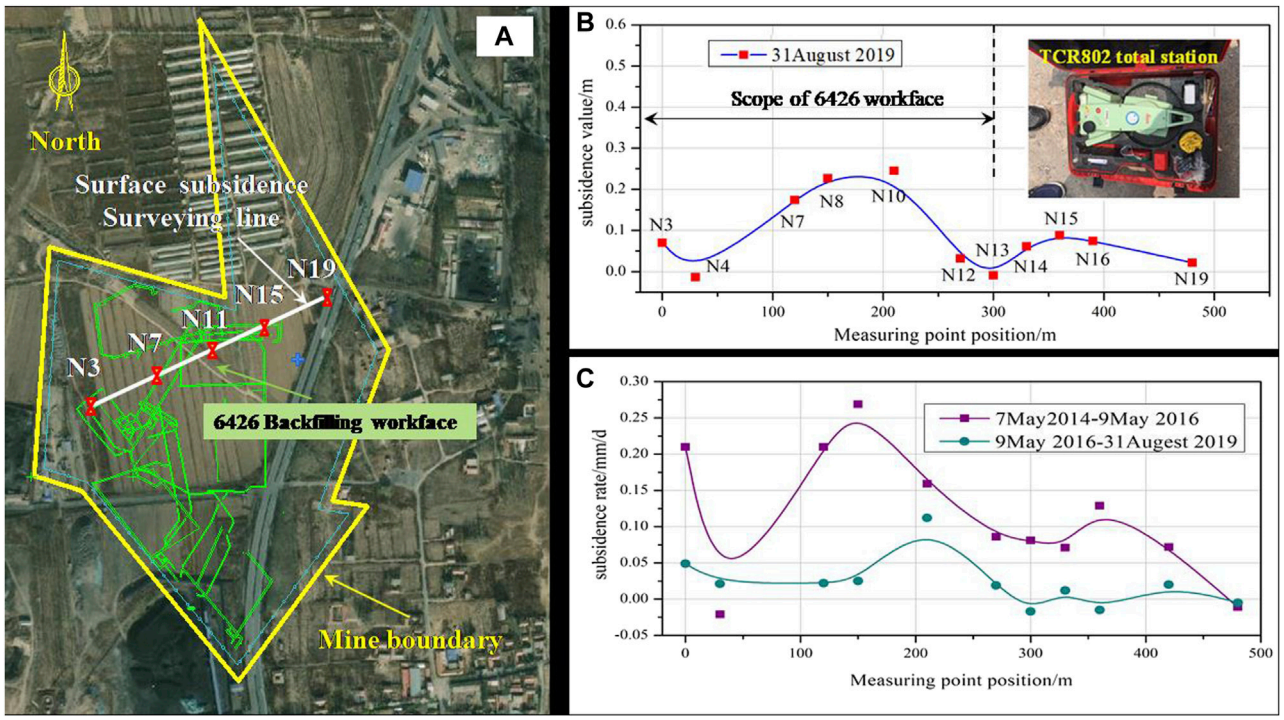

FIGURE 12 | Monitoring scheme and results of surface subsidence.

(N-A-S-H) is formed. N-A-S-H has a stronger cementing performance. In the soda residue cementing slurry system, C-S-H gel and N-A-S-H gel coexist (Liu et al., 2017), which improves the cementing performance of the system, reduces the connectivity of pores, and improves the strength of the material. This is the main reason for the gradual increases in the strength of the material with the increase in soda residue content in the range of 0–6%. The reaction process is shown in the following equation:

$$n(SiO_2{\cdot}Al_2O_3)+nSiO_2+4nH_2O \overset{OH^-}{\rightarrow} (-Si-O-Al-O-Si-O)_n. \quad (7)$$

With the continuous increase in soda residue content, the degree of soda residue participating in the hydration reaction of materials is weakened, and the surplus soda residue no longer participates in the hydration reaction. The decrease of fly ash content reduces the content of the C-S-H gel polymer and N-A-S-H polymer. Since the strength of soda residue itself is low, the strength of SRGBM shows a downward trend with the continuous increase in soda residue content.

ENGINEERING APPLICATION AND FIELD MEASUREMENT OF SURFACE SUBSIDENCE

Surface Subsidence Observation

The working face 6246 of a mine was selected as the experimental working face of soda residue cemented backfilling. According to the test results, the material ratio of Group A2 was used. Surface settlement observation points were set on the corresponding surface of the working face. Then, the surface subsidence of the backfilling working face was monitored, and the control effect of SRGBM on the surface subsidence was observed. The survey line was arranged on the north of the coal mine, and the length of the survey line was 480 m. A total of 17 measuring points (N3-N19) were arranged at an interval of 30 m. The monitoring instrument was tested by the Laika TCR802 total station. Below the survey line was the working face 6246. The surface subsidence monitoring lines were monitored on May 7, 2014, May 9, 2016, and August 31, 2019. Some observation points were damaged or lost due to human destruction and natural factors, but there are still 11 observation points in good condition. **Figure 12** presents the surveying scheme and surveying results.

As shown in **Figure 12B**, the maximum surface subsidence from May 7, 2014, to August 31, 2019, is 245 mm, which is located above the working face 6246. According to the subsidence velocity curve, from May 7, 2014, to May 9, 2016, the surface subsidence velocity is faster (the maximum subsidence velocity of measuring point N8 is 0.269 mm/d) than that from May 9, 2016, to August 31, 2019 (the maximum subsidence velocity of N10 is 0.112 mm/d). The measuring points N8 and N10 are, respectively, located above the working face 6246, and the mining of the working face 6246 is completed on December 31, 2015. It can be known that the main reason for the rapid surface subsidence from May 7, 2014, to May 9, 2016, is that

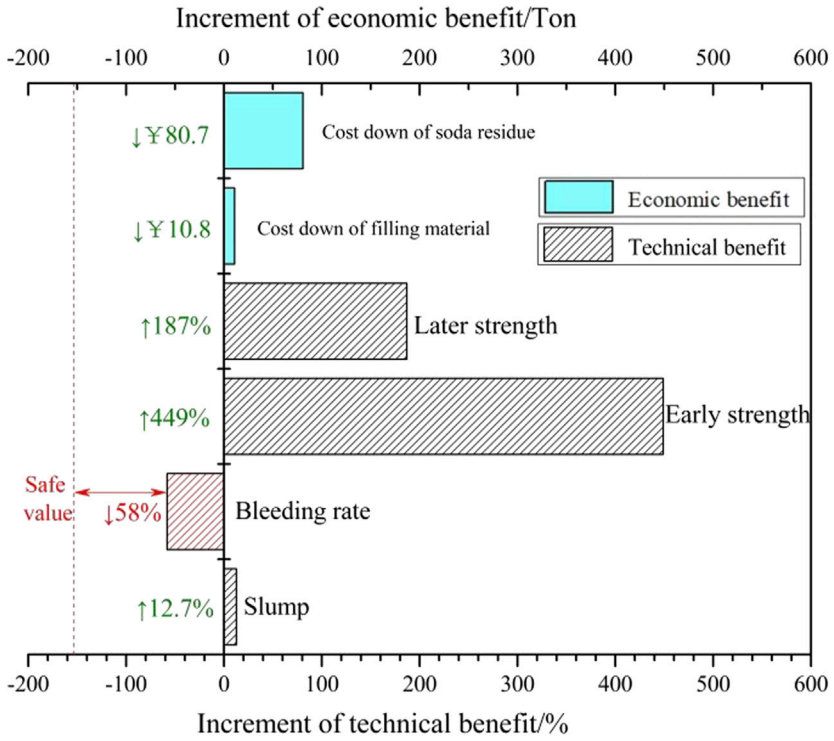

FIGURE 13 | Technical and economic benefit.

the working face 6246 is in the mining period, and the mining had a severe impact on the overlying rock, which leads to the rapid surface subsidence. During the second observation of the working face 6246, the mining has been completed, and the surface subsidence was slow. In addition, the measuring points N14, N15, and N16 are at the edge of the working face 6241. Combined with the subsidence curves and subsidence speed curves, it can be seen that the surface subsidence is small from May 9, 2016, to August 31, 2019, and the surface subsidence has tended to be stable. In summary, SRGBM has a good control effect on overburden movement and can effectively control the surface subsidence.

Benefit Analysis

The test results show that the effect of soda residue on the transport performance and mechanical properties of SRGBM is significant, and the surface subsidence value of the test mine is small, and the surface subsidence control effect is good. To comprehensively compare and analyze the influence of soda residue on the economic, technical, and social benefits of cemented fill mining, SRGBM with the soda residue content of 6% in Group A2 and SRGBM without soda residue content in Group A0 were taken as the comparison. **Figure 13** shows the specific results of data analysis.

In Group A2, 6% fly ash in Group A0 was replaced by solid waste soda residue. The results show that the performance indexes of specimens in Groups A2 and A0 are significantly improved except for the bleeding rate. The slump of SRGBM slurry increases by 12.7%. With the increase in slurry bleeding, although the increase in bleeding rate is 58%, the bleeding rate is only 3.8% (less than 5%), which still meets the engineering requirements. The increase in early strength and later strength is 449 and 187%, respectively, and the mechanical properties of SRGBM are greatly improved. According to statistics, the plant price of fly ash and soda is about 150 yuan per ton and 80.7 yuan per ton. Considering the transportation cost of soda residue, the economic benefit of SRGBM is estimated to be 200 yuan per ton of soda residue consumed. At the same time, this technology can achieve energy saving and emission reduction, environmental protection and social benefits and has good application value (Biernacki et al., 2017).

CONCLUSION

1) The moisture content of fresh soda residue is 89.95%, and the pH value is 9.2, which is alkaline. The plasticity index of fresh soda residue is 29.53, which belongs to the category of cohesive soil. The UCS of soda residue is only 0.20 MPa. Soda residue is a porous aggregate structure, with many internal interconnected pores, large compression deformation, and weak bearing capacity.
2) With the increase in soda residue content within the range of 0–12%, the slump of the SRGBM slurry gradually increases, and the bleeding rate gradually increases, but the proportion

of bleeding in the early rapid bleeding stage (stage I) is gradually smaller. The early strength, middle strength, and later strength of SRGBM increase first and then decrease. The optimum mix proportion of SRGBM is soda residue: fly ash: lime: cement: gangue = 6%: 34%: 10%: 2.5%: 47.5%, and the slurry concentration is 84 wt%.

3) Soda residue promotes the hydration reaction of cementing materials in the slurry system, and C-S-H gel and N-A-S-H gel coexist in the slurry system. The N-A-S-H gel has a stronger cementing performance, reduces the connectivity of pores, and improves the strength of materials. However, the excessive addition of soda residue cannot always promote the formation of C-S-H and N-A-S-H. The excessive addition of soda residue can reduce the strength of the material gradually.
4) The field measurement of the surface subsidence shows that the maximum subsidence value of the backfilling working face with SRGBM is only 245 mm, and the surface subsidence control effect is good. The statistical data show that compared with the reference group, the slump of SRGBM in Group A2 increases by 12.7%, the bleeding rate is only 3.8%, and the early strength and later strength increase by 449 and 187%, respectively; the economic benefit of 200 yuan is generated by the addition of soda residue per ton. The technical, economic, and social benefits of soda residue cemented filling materials are remarkable.

DATA AVAILABILITY STATEMENT

WY: Conceptualization, Data curation,Writing–original draft. KZ and SO: Design and complete experiments. XB: Complete the translation and article proofs. JZ: Polish the article and partial data analysis.

AUTHOR CONTRIBUTIONS

All authors listed have made a substantial, direct, and intellectual contribution to the work and approved it for publication.

FUNDING

This work was funded by the National Natural Science Foundation of China (Grant No: 51904110) and the Open Fund for Jiangsu Key Laboratory of Advanced Manufacturing Technology (Grant No: HGAMTL_1714).

REFERENCES

Biernacki, J. J., Bullard, J. W., Sant, G., Banthia, N., Brown, K., Glasser, F. P., et al. (2017). Cements in the 21st Century: Challenges, Perspectives, and Opportunities. *J. Am. Ceram. Soc.* 100 (100), 2746–2773. doi:10.1111/jace.14948

Cui, Z., and Henghu, S. N. (2010). The Preparation and Properties of Coal Gangue Based Sia Lite Paste-like Backfill Material[J]. *J. China Coal Soc.* 35 (06), 896–899.

Deng, X., Yuan, Z., Yu, Li., Liu, H., Feng, J., and Benjamin, W. (2020). Experimental Study on the Mechanical Properties of Microbial Mixed Backfill[J]. *Construct. Build. Mater.* 265, 120643. doi:10.1016/j.conbuildmat.2020.120643

Guangming, F., Sun, C., Wang, C., and Zhou, Z. (2010). Research on Goaf Filling Methods with Super High-Water Material[J]. *J. China Coal Soc.* 35 (12), 1963–1968. doi:10.13225/j.cnki.jccs.2010.12.004

He, Y., Ye, X., and Wang, Z. (2015). Consideration on the 13th Five Year Plan of Coal Industry[J]. *Coal Econ. Res.* 35 (01), 6–8+21. doi:10.13202/j.cnki.cer.2015.01.001

Hulisz, P., and Piernik, A. (2013). Soils Affected by Soda Industry in Inowrocaw[J]. *Techn. Soils of Poland* (7), 125–140.

Lanfen, H., Li, J., Chen, Z., and Wang, L. (2014). Effect of Combined Application of Alkali Residue and Biomass Ash on Improving Acid Soil[J]. *South China Fruits* 43 (04), 65–67. doi:10.1016/j.still.2016.04.017

Li, B., Yan, H., Zhang, J., and Zhou, N. (2020a). Compaction Property Prediction of Mixed Gangue Backfill Materials Using Hybrid Intelligence Models: A New Approach[J]. *Constr. Build. Mater.* 247, 118633. doi:10.1016/j.conbuildmat.2020.118633

Li, D., Wang, D., and Yuan, N. (2020b). Influence of Circulating Fluidized Bed Fly Ash on Properties of Gangue Cemented Filling Materials[J]. *Bull. Chin. Ceram. Soc.* 39 (08), 2401–2407+2432. doi:10.16552/j.cnki.issn1001-1625.2020.08.006

Liu, C., Zhao, X., Zhu, N., Liu, Y., and Pang, Y. (2017). Mechanical Properties of Fly Ash-Based Geopolymers and Modification Mechanism of Soda Residue[J]. *Bull. Chin. Ceram. Soc.* 36 (02), 679–685+691. doi:10.16552/j.cnki.issn1001-1625.2017.02.046

Liu, H., Zhang, J., Li, B., Zhou, N., Xiao, X., Li, M., et al. (2020). Environmental Behavior of Construction and Demolition Waste as Recycled Aggregates for Backfilling in Mines: Leaching Toxicity and Surface Subsidence Studies. *J. Hazard. Mater.* 389, 121870. doi:10.1016/j.jhazmat.2019.121870

Liu, L., Fang, Z., Zhang, B., Wang, M., Qiu, H., and Zhang, X. (2021). Development History and Basic Categories of Mine Backfill Technology[J]. *Metal Mine* 50 (03), 1–10. doi:10.19614/j.cnki.jsks.202103001

Ma, D., Wang, J., Cai, X., Ma, X., Zhang, J., Zhou, Z., et al. (2019). Effects of Height/diameter Ratio on Failure and Damage Properties of Granite under Coupled Bending and Splitting Deformation. *Eng. Fracture Mech.* 220, 106640. doi:10.1016/j.engfracmech.2019.106640

Ma, J., Zhang, P., Bai, X., and Arsyad, A. (2019). Experimental on Bearing Capacity of Alkali Slag Foundation[J]. *Sci. Tech. Eng.* 19 (30), 303–309. doi:10.28991/cej-2020-03091623

Ma, D., Duan, H., Liu, W., Ma, X., and Tao, M. (2020). Water-sediment Two-phase Flow Inrush hazard in Rock Fractures of Overburden Strata during Coal Mining. *Mine Water Environ.* 39, 308–319. doi:10.1007/s10230-020-00687-6

Ma, D., Duan, H., Zhang, Q., Zhang, J., Li, W., Zhou, Z., et al. (2020). A Numerical Gas Fracturing Model of Coupled thermal, Flowing and Mechanical Effects. *Comput. Mater. Contin.* 65 (3), 2123–2141. doi:10.32604/cmc.2020.011430

Ma, D., Zhang, J., Duan, H., Huang, Y., Li, M., Sun, Q., et al. (2021). Reutilization of Gangue Wastes in Underground Backfilling Mining: Overburden Aquifer protection. *Chemosphere* 264, 128400. doi:10.1016/j.chemosphere.2020.128400

Ma, D., Kong, S., Li, Z., Zhang, Q., Wang, Z., and Zhou, Z. (2021). Effect of Wetting-Drying Cycle on Hydraulic and Mechanical Properties of Cemented Paste Backfill of the Recycled Solid Wastes. *Chemosphere* 282, 131163. doi:10.1016/j.chemosphere.2021.131163

Martin, J., and Holger, W. (2013). Progress in the Research and Application of Coal Mining with Stowing[J]. *Int. J. Mining Sci. Tech.* 23 (1), 7–12. doi:10.1016/j.ijmst.2013.01.002

Meng, L., Zhang, J., Zhou, N., and Huang, Y. (2017). Effect of Particle Size on the Energy Evolution of Crushed Waste Rock in Coal Mines. *Rock Mech. Rock Eng.* 50 (5), 1347–1354. doi:10.1007/s00603-017-1207-1

Meng, Li., Zhang, J., Meng, G., Gao, Y., and Li, A. (2020). Testing and Modelling Creep Compression of Waste Rocks for Backfill with Different Lithologies[J]. *Int. J. Rock Mech. Mining Sci.* 125, 104170. doi:10.1016/j.ijrmms.2019.104170

Mitchell, J. K. (1993). *Foundmentals of Soil Behavior*. John Wiley&Sons Inc. 21, 43–47.

Morgan, D. R. (1996). Compatibility of concrete Repair Materials System[J]. *Constr. Build. Mater.* 10 (1), 51–61. doi:10.1016/0950-0618(95)00060-7

Papadakis, V. G. (1999). Effect of Fly Ash on Portland Cement Systems. *Cement Concr. Res.* 29, 1727–1736. doi:10.1016/s0008-8846(99)00153-2

Ran, H., Guo, Y., Guorui, F., Qi, T., and Du, X. (2020). Creep Properties of Coal Gangue Cemented Backfill Material under Step Loading[J]. *Mining Res. Develop.* 40 (02), 42–47. doi:10.13827/j.cnki.kyyk.2020.02.008

Shenyang, O. (2019). *Study on Transportation and Mechanical Properties Optimization of Sand-Based Cemented Filling Materials[D]*. XuZhou: China University of Mining and Technology

Song, Q., Liu, K., Fu, X., and Li, H. (2019). New Technology of Rock Salt Mining by Filling-Water Solution[J]. *China Well Rock Salt* 50 (04), 19–21.

Sun, S., Zheng, Q., Tang, J., Zhang, G., Zhou, L., and Shang, W. (2012). Experimental Research on Expansive Soil Improved by Soda Residue[J]. *Rock Soil Mech.* 33 (06), 1608–1612. doi:10.16285/j.rsm.2012.06.045

Tan, A., Lianyu, W., and Wang, Q. (2018). Physical and Mechanical Experimental Study on Improving Weathered Mudstone with Soda Residue[J]. *Bull. Chin. Ceram. Soc.* 37 (08), 2610–2615. doi:10.16552/j.cnki.issn1001-1625.2018.08.044

Tian, X., and Li, X. (2009). Research on Engineering Utilization of Soda Residue Soil in Tangshan.[J]. *Build. Sci.* 25 (07), 77–79+101.

Wang, T., Wang, Z., Wang, S., Pan, Y., and Kang, Y. (2014). Study on Flowing Features of Mine High Density Cemented Filling Slurry in Pipeline[J]. *Coal Sci. Tech.* 42 (S1), 50–52. doi:10.13199/j.cnki.cst.2014.s1.035

Wang, C., Liu, Y., Hu, H., Li, Y., and Lu, Y. (2019). Study on Filling Material Ratio and Filling Effect: Taking Coarse Fly Ash and Coal Gangue as the Main Filling Component. *Adv. Civil Eng.* 2019 (1), 1–11. doi:10.1155/2019/2898019

Wang, M. (2019). Simulation experiment of Coupling Effect between Surrounding Rock and Filling Body in Early Strength Stage[J]. *J. Wuhan Univ. Sci. Tech.* 42 (02), 129–134.

Xu, D., Wen, N., Wang, Q., Xu, C., and Jiang, Y. (2020). Preparation of Clinker-free concrete by Using Soda Residue Composite Cementitious Material[J]. *J. Harbin Inst. Tech.* 52 (08), 151–160.

Yan, S., Hou, J., and Liu, R. (2006). Research on Geotechnical Properties and Environmental Effect of Mixture of Soda Waste and Fly Ash[J]. *Rock Soil Mech.* 27 (12), 2305–2308. doi:10.16285/j.rsm.2006.12.042

Yang, J., Wu, X., Zhang, L., He, C., and Bao, G. (2010). Study on Experimental Preparation of Cement Mortar Incorporating Fly Ash-Soda Residue[J]. *Bull. Chin. Ceram. Soc.* 29 (05), 1211–1216. doi:10.16552/j.cnki.issn1001-1625.2010.05.045

Yang, Y., Pu, Y., Yan, W., GuoO, W., and Wang, H. (2017). Microstructure and Chloride Ion Dissolution Characteristics of Soda Residue[J]. *J. South China Univ. Tech.* 45 (05), 82–89.

Yang, Y., Pu, Y., Yan, W., Guo, W., and Wang, H. (2017). Experimental Study on the Performance of concrete Using Soda Residue as mineral Admixture[J]. *Concrete* (09), 80–83.

Yin, L., Wang, H., Guo, H., Li, H., Wang, K., and Wu, H. (2020a). Proportion Optimization and Performance of Filling Materials with Large-Content of Fly Ash [J]. *Mining Res. Develop.* 40 (03), 56–61. doi:10.13827/j.cnki.kyyk.2020.03.013

Yin, S., Shao, Y., Wu, A., Wang, H., Liu, X., and Wang, Y. (2020b). A Systematic Review of Paste Technology in Metal Mines for Cleaner Production in China. *J. Clean. Prod.* 247, 119590. doi:10.1016/j.jclepro.2019.119590

Yu, W., Qi, Y., Zhou, Y., Chen, L., Du, H., and Xie, H. (2016). Synergistic Improvement of thermal Transport Properties for Thermoplastic Composites Containing Mixed Alumina and Graphene Fillers[J]. *J. Appl. Polym. Sci.* 133 (13), 4830. doi:10.1002/app.43242

Zhang, J., Zhang, Q., Ju, F., et al. (2018). Theory and Technique of Greening Mining Integrating Mining, Separating and Back Filling in Deep Coal Resources [J]. *J. China Coal Soc.* 43 (2), 377–389. doi:10.13225/j.cnki.jccs.2017.4102

Zhang, J., Ju, F., Meng, L. I., et al. (2020). Method of Coal Gangue Separation and Coordinated *In-Situ* Backfill Mining[J]. *J. China Coal Soc.* 45 (1), 131–140. doi:10.13225/j.cnki.jccs.YG19.1826

Zhao, K., Wang, X., Liu, H., Wu, C., and Zhang, J. (2011). Experimental Study of Mechanical Behaviors of Cemented Tailings Backfill Roof with Reinforcement [J]. *Rock Soil Mech.* 32 (01), 9–14+20. doi:10.16285/j.rsm.2011.01.001

Zhou, N., Ma, H., Ouyang, S., Germain, D., and Hou, T. (2019). Influential Factors in Transportation and Mechanical Properties of Aeolian Sand-Based Cemented Filling Material[J]. *Minerals* 9 (2), 116. doi:10.3390/min9020116

Conflicts of Interest: Authors WY and KZ were employed by Huai'an Zhongbo Traffic Safety Technology Co. Ltd.

The remaining authors declare that the research was conducted in the absence of any commercial or financial relationships that could be construed as a potential conflict of interest.